Mean Value Modelling of a Diesel Engine with Turbo Compound

Master's thesis
performed in **Vehicular Systems**

by
Oscar Flärdh and Manne Gustafson

Reg nr: LiTH-ISY-EX-3443-2003

19th December 2003

Mean Value Modelling of a Diesel Engine with Turbo Compound

Master's thesis

performed in **Vehicular Systems**,
Dept. of Electrical Engineering
at **Linköpings universitet**

by **Oscar Flärdh and Manne Gustafson**

Reg nr: LiTH-ISY-EX-3443-2003

Supervisor: **Jonas Biteus**
          Linköpings universitet
          David Elfvik
           Scania CV AB
          Mattias Nyberg
           Scania CV AB

Examiner: **Associate Professor Lars Eriksson**
          Linköpings universitet

Linköping, 19th December 2003

Titel   Medelvärdesmodellering av en dieselmotor med kraftturbin

Title   Mean Value Modelling of a Diesel Engine with Turbo Compound

Författare   Oscar Flärdh and Manne Gustafson
Author

Sammanfattning
Abstract

Over the last years, the emission and on board diagnostics legislations for heavy duty trucks are getting more and more strict. An accurate engine model that is possible to execute in the engine control system enables both better diagnosis and lowered emissions by better control strategies.

The objective of this thesis is to extend an existing mean value diesel engine model, to include turbo compound. The model should be physical, accurate, modular and it should be possible to execute in real time. The calibration procedure should be systematic, with some degree of automatization.

Four different turbo compound models have been evaluated and two models were selected for further evaluation by integration with the existing model. The extended model showed to be quite insensitive to small errors in the compound turbine speed and hence, the small difference in accuracy of the tested models did not affect the other output signals significantly. The extended models had better accuracy and could be executed with longer step length than the existing model, despite that more complexity were added to the model. For example, the mean error of the intake manifold pressure at mixed driving was approximately 3.0%, compared to 5.8% for the existing model. The reasons for the improvements are probably the good performance of the added submodels and the systematic and partly automatized calibration procedure including optimization.

Abstract

Over the last years, the emission and on board diagnostics legislations for heavy duty trucks are getting more and more strict. An accurate engine model that is possible to execute in the engine control system enables both better diagnosis and lowered emissions by better control strategies.

The objective of this thesis is to extend an existing mean value diesel engine model, to include turbo compound. The model should be physical, accurate, modular and it should be possible to execute in real time. The calibration procedure should be systematic, with some degree of automatization.

Four different turbo compound models have been evaluated and two models were selected for further evaluation by integration with the existing model. The extended model showed to be quite insensitive to small errors in the compound turbine speed and hence, the small difference in accuracy of the tested models did not affect the other output signals significantly. The extended models had better accuracy and could be executed with longer step length than the existing model, despite that more complexity were added to the model. For example, the mean error of the intake manifold pressure at mixed driving was approximately 3.0%, compared to 5.8% for the existing model. The reasons for the improvements are probably the good performance of the added submodels and the systematic and partly automatized calibration procedure including optimization.

Keywords: mean value engine modelling, turbo compound, calibration, parameter setting, modularity

Outline

Chapter 1 gives a general background to the thesis and also describes the objectives and the delimitations.

Chapter 2 describes the system being modelled, a diesel engine.

Chapter 3 intend to explain the the working process. In addition, the measurement setup is described. Criticism towards the chosen method is also presented.

Chapter 4 starts with a description of the existing model. After that, four different turbo compound models are presented.

Chapter 5 describes the parameter setting process.

Chapter 6 presents the performance of the models. First, the turbo compound models are validated by them selves. Then two of the models are added to the existing model, and the new extended models are validated.

Chapter 7 presents the conclusions and discusses possible extensions.

Acknowledgment

We would like to thank our supervisors at Scania, David Elfvik and Mattias Nyberg and our supervisor at Linköpings universitet, Jonas Biteus, for inspiring discussions that have brought the work forward. Our examiner Lars Eriksson have also contributed to the thesis work, particularly by providing the optimization package used for calibration. Also, a special thanks to Jesper Ritzén, whose experience in engine modelling and measurements in vehicle at Scania have been to great help. He has also, together with the rest of the people at the departments NEE and NEP, contributed to the work by making our stay at Scania and Södertälje a pleasant experience. We are also very thankful for the help we have got from people at Scania not mentioned here, without them this thesis had not been possible to accomplish.

Oscar Flärdh and Manne Gustafson
Södertälje, December 2003

Contents

Chapter 1

Introduction

This master's thesis was performed at Scania CV AB in Södertälje. Scania is a worldwide manufacturer of heavy duty trucks, busses and engines for marine and industrial use. The work was carried out at the engine software development department, which is responsible for the engine control and the on board diagnostics (OBD) software. OBD is a system for online detection of faults.

1.1 Background

Over the latest years, the emission legislations on heavy duty trucks are getting more and more strict. One way to lower the emissions is to use better and more advanced engine control systems. This can be achieved by using model based control.

Besides the emission legislation, there is also a new OBD legislation. This means that every new truck must have an OBD system that fulfils certain demands. For example, it must be able to detect any fault that causes emission levels higher than the legislative limits. To achieve this, model based diagnosis can be used. By having models describing the fault free case, it is possible, for example to, detect deviations between the fault-free value from the model and the value from a sensor. A more accurate model can detect smaller deviations and thereby improve diagnosis performance.

In addition to control and diagnosis, there are many other areas where models can be used. For example, they can be used for different simulations, such as implementing a fault into the model and see how it will affect the system. Models can also be used for other development purposes, like testing a new control strategy. Yet another application for models is to complement sensors.

1

1.1.1 Existing Work

As seen above, models have a wide area of use and therefore they are of interest for Scania. There are many types of engine models, describing different phenomena. In this thesis, focus will be on mean value engine models. In such a model, all signals are mean values over one or several cylinder cycles [10].

At Scania, some mean value engine modelling has already been done. David Elfvik [3] began the work by producing a physical model, and several people has developed and extended it. After the work done by Jesper Ritzén [12], the model fulfilled the demand on accuracy and real time executability. In this case, real time executable means that the model can be simulated at 10 milliseconds fixed step length. This is because the engine control system, S6, executes in cycles of 10 milliseconds.

1.2   Problem Formulation

Even though the previous modelling at Scania has reached far, there is still work to do. None of the models include turbo compound, which means that there is no model for such engines. Thus there is a desire to extend the existing model with turbo compound, and still have a physical, accurate and real time executable model. A model being physical means that the structure of the model is based on the physical relations.

There are several reasons for having a physical model instead of a blackbox model. One reason is that there is not much theory on nonlinear dynamic blackbox modelling. Another reason is that a physical model is often better at extrapolation. When developing a blackbox model, one must in some cases still find the physical principles to find the inputs. With a physical model, it is also possible to add outputs afterwards. Yet another reason for a physical model is that it is possible to implement faults (other than input faults) and simulate for diagnosis purposes.

To make it easy to develop the model and extend it with different components, it is desirable that the model is modular. It should be easy to switch between different submodels for the same component or to add new submodels. A systematic way to determine the parameters in the model would make the maintenance easier. Some degree of automatization in this process would also be beneficial.

1.3 Objectives

The objectives of this thesis is to extend the existing mean value engine model at Scania with a turbo compound model. The complete engine model should be:

- Physical
- Accurate
- Real time executable
- Modular

The parameter tuning should be systematic, with some degree of automatization.

1.4 Delimitations

The exhaust brake that the engine is equipped with is not modelled. During calibration and validation, the periods of time when the exhaust brake was active, has been excluded.

The equations of the existing model will not be changed. Only the structure and implementation of the model and the parameter setting will be changed.

1.5 Target Group

The target group of this thesis is mainly people working at Scania CV, undergraduate and graduate science students. Knowledge in vehicular systems, fluid mechanics and thermodynamics increases the understanding.

Chapter 2

The Diesel Engine

In this chapter the basic operation of the turbocharged diesel engine will be described, furthermore, turbo compound is described more deeply. The chapter is intended to increase the understanding of the thesis for readers who are not familiar with the diesel engine and its components.

2.1 The Turbocharged Diesel Engine

The operating principle of an internal combustion engine is to mix air with fuel and burn it to generate work. The amount of air limits the fuel quantity that can be combusted. The more air the more oxygen, and more oxygen means that more fuel can be combusted and generate work.

In figure 2.1, the main components in the air and exhaust path are shown. First, the air is cleaned by the air filter. After that, a compressor raises the pressure of the air. But the temperature is also raised, hence an intercooler is used. The air is cooled by air streams from the ambient air caused by vehicle movement and a fan. By the use of both a compressor and an intercooler, the pressure is raised but the temperature is nearly the same. This means that the density of the air is increased. The compressed air then enters the cylinders via the intake manifold. The increased air density now enables more fuel to be combusted.

In the cylinders, the combustion process takes place. All engines at Scania are four stroke compression ignited engines. The combustion process follows four strokes:

- The intake stroke, where the air in the intake manifold is inducted into the cylinder.
- The compression stroke, where the air is compressed due to the piston movement. During the compression stroke, the diesel is injected. Due to the high compression, it ignites.
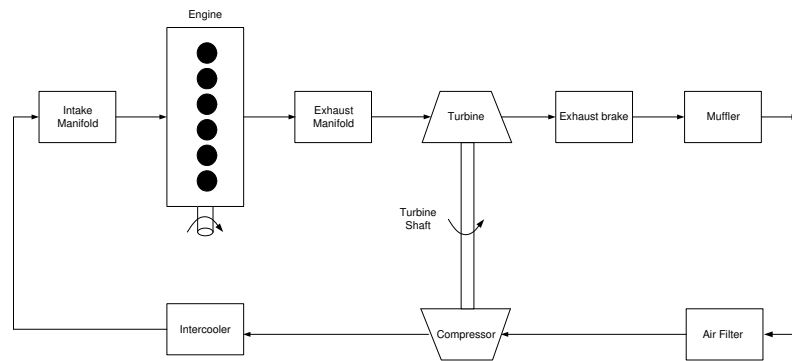
Figure 2.1: The main components of the conventional diesel engine.

- The expansion stroke, where the high pressure generated by the combustion produces work by pushing down the piston.

- The exhaust stroke, where the burned air/fuel mixture exits the cylinder into the exhaust manifold.

Totally, these four strokes takes two engine revolutions, which mean that an n cylinder engine has $n/2$ intakes and $n/2$ exhaust strokes per engine revolution.

The high pressure and temperature in the exhaust manifold drives the primary turbine, which is connected to the compressor via the turbine shaft. This means that the energy in the exhaust gases is used for pushing more air into the cylinders, which is the purpose of turbocharging. After the turbine there is the exhaust brake, which is a throttle that can be used for choking the flow and thereby increases the motor brake. For example, it can be used by the driver in downhill driving to spare the brakes. The exhaust brake is followed by the exhaust system, which includes the muffler.

2.2   Turbo Compound

A turbo compound is placed after the primary turbine, and consists of a turbine, a shaft, a hydraulic coupling and gears. The compound turbine works in the same way as the primary turbine, and is connected to the hydraulic coupling via the shaft and cog wheel transmission. The hydraulic coupling is then connected to the crankshaft via cog wheel transmission.

The purpose of turbo compound is to use the energy in the exhaust gases, which drives the turbine and thereby generates torque. The torque is then transmitted to the crankshaft via the hydraulic coupling and gears.

2.2.1   The Hydraulic Coupling

The hydraulic coupling consists of two enclosed coupling halves filled with oil. Each of the halves also has a number of radial blades. One of the coupling half is connected with the crankshaft, the other with the turbine. A photo of a coupling half can be seen in figure 2.2. The reason to use a hydraulic coupling

Figure 2.2: Photo of a hydraulic coupling half.

is because of its ability to transmit torque and damp oscillations. In this case it is the oscillations on the crankshaft, generated by the combustion process, that have to be damped. The combustion in each cylinder generates a torque peak, which causes the crankshaft to oscillate.

The torque is transmitted by the oil flow in the coupling. In figure 2.3 and figure 2.4 the different flow components can be seen. The coupling half with the fastest rotating speed is called the impeller, the other is called turbine. The radial flow is caused by the rotation of the impeller. Due to the shape of the coupling half, there will also be an axial flow from the impeller to the turbine. Since the impeller rotates faster, there will be a combined tangential and axial flow that will impact the turbine blades. It is this impact force that generates the torque. Hence, a difference in rotation speed is necessary for torque transmission. The relative speed difference between the impeller and the turbine is called slip.
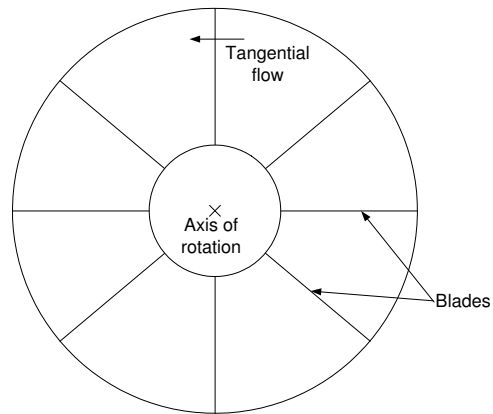
Figure 2.3: Schematic illustration of a coupling half.
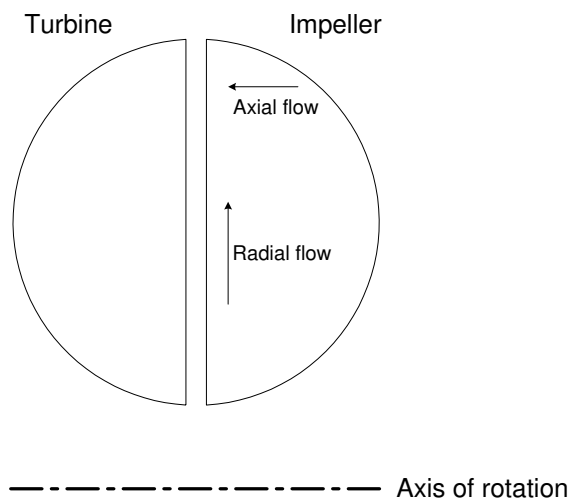
Figure 2.4: Schematic illustration of the axial and radial flow in the hydraulic coupling.

Chapter 3

Method

In this chapter, the working process in general and the measurements in particular will be described. Criticism towards the method used in the process is then discussed.

The results and conclusions are products of the working process, which means that the explanations behind a specific piece of result can be found somewhere in the process leading to it. With this approach, it is crucial to the reliability, not only to report the results, but also to describe how the results were attained. A thorough description of the working process makes it possible for the reader to review the results critically and consequently the reliability of the results can be judged.

Besides that, the description of the method is central to obtain reliability, it can also help others to extend the work presented in this thesis, to avoid the mistakes we have made and to make use of the successful parts.

3.1   Working Process

The working process leading to this master's thesis can be described by seven main activities:

Study of theory and earlier work Earlier works, for example scientific articles, master's thesis and licentiate thesis, on topics similar to the one examined in this thesis, were studied. In addition, theoretic literature concerning the physical phenomena relevant for this thesis were studied.

Modelling Equations for the component of interest are formed with the knowledge gained from the studying of the theory and earlier works as input.

Implementation The equations from the modelling phase are implemented in the Matlab toolbox Simulink.

Parameter setting The parameters in the implemented model are tuned to minimize the difference between the simulated signals and the modelling data.

Validation The simulated signals are compared to a set of measured signals, that is different from the one used for modelling.

Design of measurement setup Upon the knowledge gained from the study phase, a set of sensors and equipment for signal processing and data collection is designed.

Measurement Measurement of signals in a vehicle.

The activities have been performed one or several times during the process, which is depicted schematically in figure 3.1. The process started with study of theory and earlier works. After the first reading phase, the design of the measurement setup was done and the measurements started. Then, the measured signals were analyzed and if necessary, the design of the measurement setup were changed. In parallel to the design of the measurement setup and the measurement, the modelling activity started and was followed by the implementation. The implemented model was then validated and, furthermore, the results were analyzed. If the result was good enough, the process was ended and if the result was not to satisfaction, the procedure was repeated from the study or modelling phase until satisfaction.
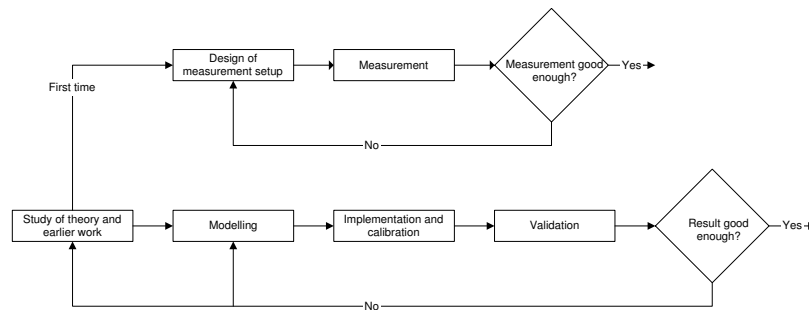
Figure 3.1: Schematic illustration of the working process.

3.2 Measurement

Measurements were performed in a vehicle. Signals from both sensors specially installed for modelling purpose and standard production sensors were used. Data from both sensor types were collected by the same measurement system. Some of the signals were processed both before and after sampling, while other were processed only after sampling. The quantities measured

were pressure, temperature and turbine speed. Below, the complete measurement setup will be described in general, and further, the measurement of the different quantities and the signal processing will be described.

3.2.1   Measurement Setup

The measurement setup is illustrated in figure 3.2. To collect the measurement data, ATI Vision measurement system was used. The system makes it possible to collect data from both external sensors and the engine control system at the same time base. One analogue and one thermocouple measurement module were used, to which breakout boxes for signal input are connected. The signals from the analogue and thermocouple modules are connected to a hub via CAN (Control Area Network). The hub is also collecting data from the engine control system via CAN and distributes it to a laptop via USB. The laptop is used for storing data and as an interface for communication with the engine control system.

The analogue measurement module have four fast channels with a minimum sample time of one millisecond and 12 slower channels with a minimum sample time of ten milliseconds. The measurement range of each channel can be switched between -5 to 5 V and -20 to 20 V. The analogue signal is converted to a 13-bit digital number, which gives a resolution of approximately 0.2 per mille of the measurement range.

The thermocouple measurement module has 16 channels and a minimum sample time of 0.2 seconds. The resolution is $0.1\,^\circ C$.

Unfortunately, non of the measurement modules is equipped with an anti-aliasing filter, hence it would have been good to use external analogue filters. The available equipment was not possible to use in the vehicle, and consequently this was not done. Instead the signals were sampled and filter afterwards. To find appropriate sample times, the signals were sampled as fast as possible and signal frequencies were analyzed using FFT (Fast Fourier Transform). The frequency analysis showed that the frequencies over the Nyquist frequency of the sample frequency used in the measurements were insignificant. Of course, no frequencies above the Nyquist frequency of the fastest sampling (one millisecond) can be detected.

3.2.2   Measured quantities

In this section, the measurement of the different quantities will be described in terms of what sensors that have been used, the quality of the measurement signal and the positioning, accuracy and response times of the sensors.

ATI VISION INTERFACE

	CAN		

CAN MODULE EDAQ 16AI+

CAN

ATI VISION NETWORK HUB

CAN

Engine control system - S6

USB

Laptop

CAN

Thermocouples 16 UNIVERSAL CHANNELS

Breakoutbox

coaxial cable

Breakoutbox EDAQ 16T

Conversion - frequency to D.C. voltage

coaxial cables

coaxial cables

coaxial cable

Ambient thermoelement

Conversion - sine to square

K-element wires

Kistler amplifiers

Scania amplifiers

Cab

coaxial cable

Kistler cable

Scania measurement cable

Engine

Thermoelements

Revolution sensors

Kistler pressure sensors

Schaevitz gauge pressure sensor

Figure 3.2: Schematic illustration of the measurement setup.

Pressure Measurement

All sensors are mounted perpendicular to the flow and consequently it is the static pressure that is measured. The measured pressures are presented in table 3.1.

The sensors used are Kistler pressure sensors, which are fast. This means that they can measure frequencies up to at least 30 kHz. They are designed for pressure measurement in dirty and warm (up to 140 $^\circ C$) environments. As some points of measurement are even warmer than 140 $^\circ C$, thin pipes are installed between the sensor and the point of measurement to protect the sensor.

The uncertainty of the sensors is $\pm 0.4\%$. Each sensor has a specific amplifier box with an output of one volt per bar, that is calibrated together with the sensor at delivery. Two different Kistler models with two different measurement ranges (5 bar and 10 bar) were used: 4045A5 and 4045A10. [8]

Note that there are two exhaust manifold pressures measured, one for each

Table 3.1: Measured pressures in vehicle

Pressure	Description	Sensor
p_{amb}	Ambient pressure [bar]	From S6
p_{im}	Inlet manifold pressure [bar]	Kistler 4045A10, 10 bar
p_{em1_1}	Exhaust manifold pressure 1 [bar]	Kistler 4045A10, 10 bar
p_{em1_2}	Exhaust manifold pressure 2 [bar]	Kistler 4045A10, 10 bar
p_{em2}	Pressure between turbines [bar]	Kistler 4045A10, 10 bar
p_{es}	Exhaust system pressure [bar]	Kistler 4045A5, 5 bar

cylinder bank. The resulting exhaust manifold pressure is considered as the mean value of these.

Temperature Measurement

For temperature measurement, thermoelements of type K was used. The measurement range of the K-element is 253 to 1423 K and the accuracy is $1.3K$ in the range up to $415K$ and $\pm 0.3\%$ in the range over $415K$[2]. The thermoelements were mounted with as large space as possible between the pipe wall and the measurement point and when possible the thermoelements have been mounted with the tip towards the flow. A list of the measured temperatures can be found in table 3.2. Note that there are two exhaust gas temperatures measured, one for each cylinder bank. The resulting exhaust manifold temperature is considered as the mean value of these.

On the intake side, where the temperatures are proportionately low, elements without encapsulation were used. For measurement of the much higher temperatures on the exhaust side of the engine, three millimeter encapsulations are used to protect the thermoelements. The encapsulation implies that the time constant is as large as 1.2 seconds, which is much slower than without encapsulation. The temperature of the exhaust gas is highly dependent on the fuel injected in the cylinder. The injected fuel can change very quickly (every cylinder cycle) and consequently the temperature of the exhaust gases do as well. The dynamics of the exhaust temperature is thus much faster than the dynamics of the encapsulated thermoelement.

Also, there are other problems when measuring temperature. The measured temperature is not only affected by the temperature of the gas, but also by radiation from the pipe walls, heat conduction through the encapsulation and friction of the particles hitting the encapsulation. For measurement of exhaust gas temperature, the radiation from the pipe walls has previously shown to be of importance [15].

Together the above problems make the measured values very uncertain and if we had been aware of them earlier in the working process we would have done the measurement differently. For example radiation shields and thinner encapsulations could have been used.

Table 3.2: Measured temperatures

Temperature	Description	Sensor
T_{amb}	Ambient temperature [K]	Thermoelement, type K
T_{im}	Inlet manifold temperature [K]	Thermoelement, type K
T_{em1_1}	Exhaust manifold temperature 1 [K]	Thermoelement, type K
T_{em1_2}	Exhaust manifold temperature 2 [K]	Thermoelement, type K
T_{em2}	Temperature between turbines [K]	Thermoelement, type K
T_{es}	Exhaust system temperature [K]	Thermoelement, type K

Turbine and Engine Speed Measurement

Two turbine speeds were measured: the speed of the primary turbine and the speed of the compound turbine. For measurement of the primary turbine speed, a Holset induction revolution sensor is used. A magnetic nut that rotates with the turbine shaft is mounted. When the turbine shaft rotates, the magnetic nut generates a magnetic field that induces a voltage in the revolution sensor. For measurement of the compound turbine speed, an inductive sensor was installed on the gear between the turbine and the hydraulic coupling. The sensor consists of a coil with a magnetic core. When a cog passes the sensor, the magnetic field in the vicinity of the sensor is changed and a voltage pulse is generated. With knowledge of the number of cogs per revolution, the turbine speed can be calculated.

The signal pulses from both the revolutions sensors were very noise and were therefore converted to square waves using a pulse converter, for easier detection. Further, the square waves were converted to a direct-current voltage proportional to the frequency using frequency/voltage converter designed and produced by Scania. The direct-current voltage were still noisy, but this was handled by software filtering (see section 3.2.3).

Table 3.3: Other signals measured

Variable	Description	Sensor
n_{trb1}	Primary turbine speed [rpm]	Holset revolution sensor
n_{trb2}	Compound turbine speed [rpm]	Inductive sensor
n_{eng}	Engine speed [rpm]	From S6

3.2.3 Signal Processing

Two kinds of filtering have been used; median filtering and low-pass filtering.

The median filter was used to suppress outliers. Each value in the filtered signal is the median value of a filter window. The filter window is defined by a specified number of values centered about the current value. Hence outliers are suppressed, but the filter also distort the original signal by suppressing

some fast variations. The wider the filtering window, the greater the distortion, but also better suppression of several outliers in a row. Primarily the turbine speed signals and the pressure signals on the exhaust side of the engine were median filtered, because these signals had outliers. One reason for this is that the magnetic field variations, that trigs the turbine speed sensors occasionally is to weak. Another reason could be that Vision has problem logging as many signals as we were interested in.

The low-pass filter is used partly to suppress measurement noise and partly to smooth the signal to fit for mean value purpose. The mean value modelling approach implies that variations faster than a few cylinder cycles are not relevant. Therefore, all the pressures on the exhaust side were filtered, using a low-pass Butterworth filter with cut off frequency 2.5 Hz to suppress the pressure pulses from the cylinder strokes. The pulsating pressures gives pulsation in the turbine speeds, hence, the turbine speeds were also low-pass filtered. The pressures on the intake side of the engine does only have small pulsation effects, but to be safe and reduce noise, all the pressures were low-pass filtered. Also, the ambient pressure, which is an input signal to the model, had to be filtered, but for an other reason. The signal had quite large resolution, which gave unphysical behavior.

3.3   Method Criticism

The intention of this section is not to point everything that may have affected the study in a negative way. A discussion like that would never be complete, and the reliability judgment is left to the reader. Still there are some details we want to emphasize.

The working process contains lots of subjective choices, for example choice of literature to study, what filtering, sensors and points of measurements to use, etc. It is very unlikely that someone else would have done exactly the same choices. The choices have of course affected the result, which implies that if somebody else would have performed the study, the result would probably have been different. The intention has been to describe the method used and the considerations and assumptions made. This, to make it possible for the reader to evaluate the results and use the results in the appropriate applications.

The study has been carried out with measurement data from only one vehicle. Even though there are a lot of similarities between different engine and vehicle models, there are a lot of differences as well. An adaptation of the model to another engine model should, as far as we can judge, not imply problems. Still, the work has only been performed on one engine.

To that, two specific problems that, with no doubt, have affected the result negatively are the relatively bad exhaust temperature model and large uncertainty of the temperature measurement. Together, these make it hard to perform a fair evaluation of the rest of the model. This, because many of the

other quantities modell are dependent on the simulated temperatures. If the measured temperatures had been reliable, the rest of the modelled could have been validated with use of these. Not even that was possible, due to the wall radiation effects and bad response times.

Chapter 4

Modelling

This chapter intend to describe the modelling of the different components. First, the existing model will be described briefly and then the compound models are presented. Thereto, the turbo compound model is combined with the existing model forming an extended model. Also, the modular implementation of the model is discussed.

4.1 Existing Model

In this section, the existing mean value engine model at Scania will be described briefly. The model is for a turbocharged diesel engine without turbo compound and exhaust brake. It has been developed in several steps by combining submodels earlier presented in the master's theses [13] [11], engine modelling literature [6] and others [5]. The final steps in the development of the model was taken by David Elfvik [3] and Jesper Ritzén [12] in their master's theses. Thus, the equations presented below have not been chosen or developed by us. Still, they are crucial to the general understanding of the engine model and the problems associated with integrating the new submodels with the existing model. The different submodels will be presented following the air/exhaust path through the engine, starting from the intake side. An illustration of the model can be found in figure 4.1 and the inputs and outputs can be seen in figure 4.2.

4.1.1 Compressor

The first component in the air path that is modelled is the compressor, which is stiffly connected to the turbine via the turbine shaft. The modelling of the turbine and the turbine shaft is presented in section 4.1.5 and 4.1.6. Earlier, this model has been presented in [5]. Two output signals are of interest; the

torque produced by the compressor and the mass flow through the compressor. The torque is given by:

$$\tau_{cmp} = \frac{W_{cmp}c_{p_{air}}T_{amb}}{\eta_{cmp}\omega_{cmp}} \left(\left(\frac{p_{im}}{p_{amb}} \right)^{\frac{\gamma_{air}-1}{\gamma_{air}}} - 1 \right) \qquad (4.1)$$

The flow and the efficiency is modelled by maps provided by the manufacturer. The pressure ratio over and the speed of the compressor are inputs to the maps.

$$W_{cmp} = f_{W_{cmp}} \left(\frac{p_{im}}{p_{amb}}, n_{cmp} \right) \qquad (4.2)$$

$$\eta_{cmp} = f_{\eta_{cmp}} \left(\frac{p_{im}}{p_{amb}}, n_{cmp} \right) \qquad (4.3)$$
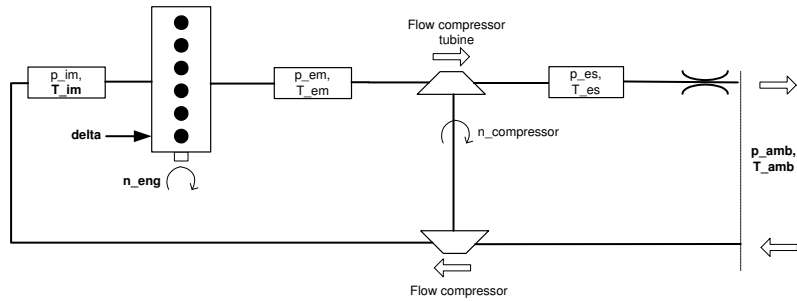

Figure 4.1: Schematic illustration of the existing model, input signals are bold.
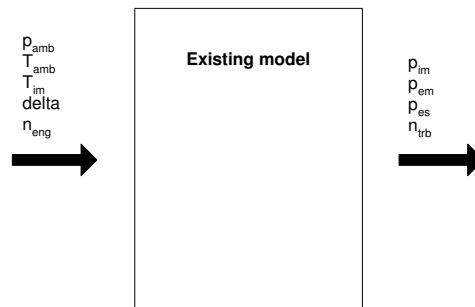

Figure 4.2: Input and output signals of the existing model.

4.1.2 Intake Manifold

The intake manifold is modelled using a standard control volume, earlier described in for example [1] and [3]. The control volume equations is derived by differentiating the ideal gas law:

$$\dot{p} = \frac{\dot{m}RT}{V} + \frac{mR\dot{T}}{V} \tag{4.4}$$

This approach will give two states, but by applying the assumption that the temperature varies slowly the number of states is reduced to one. This assumption is earlier suggested in [15], but without further motivation. The resulting equation, and the one used in the model is:

$$\dot{p} = \frac{\dot{m}RT}{V}, \tag{4.5}$$

where $\dot{m}$ is given by the difference between $W_{im_{in}}$ and $W_{im_{out}}$. The flow through the compressor is considered as $W_{im_{in}}$ and the flow into the engine is considered as $W_{im_{out}}$. Consequently, the state equation for the intake manifold is given by 4.6, with V_{im} as the only parameter.

$$\dot{p}_{im} = \frac{R_{air}T_{im}(W_{cmp} - W_{eng_{in}})}{V_{im}} \tag{4.6}$$

4.1.3 Engine

The engine submodel consists of two submodels, one for the flow through the engine and one for the temperature of the exhaust gases.

Engine Flow Model

During the intake phase of the cylinder cycle, air fills the cylinders. The air mass flow into the engine depends on many different factors, but the most important are engine speed, intake manifold pressure and temperature. Volumetric efficiency, η_{vol}, is the ratio between the mass inducted into the engine and mass ideally inducted (the displaced volume every cylinder cycle). The air mass flow into the engine is ideally:

$$\dot{m}_{ideal} = \frac{V_d n_{eng} p_{im}}{2RT_{im}} \tag{4.7}$$

Consequently the actual amount inducted into the engine is:

$$\dot{m} = \eta_{vol} \frac{V_d n_{eng} p_{im}}{2RT_{im}} \tag{4.8}$$

The volumetric efficiency is mapped from the engine speed and the intake manifold temperature.

$$\eta_{vol} = f_{\eta_{vol}}(n_{eng}, T_{im}) \tag{4.9}$$

During the exhaust phase, the exhaust gases are pressed out of the cylinder and into the exhaust manifold. The flow out of the engine equals the sum of the flow into the engine and the amount of fuel injected.

$$W_{eng_{out}} = W_{eng_{in}} + W_{fuel}, \tag{4.10}$$

where

$$W_{fuel} = \frac{\delta n_{eng} N_{cyl}}{120} \tag{4.11}$$

Exhaust Gas Temperature

The exhaust gas temperature is modelled as an ideal Otto cycle and is earlier presented in [13]. A non-linear equation system has to be solved in every time step. The equations are:

$$T_{em} = T_1 \left(\frac{p_{em}}{p_{im}}\right)^{\frac{\gamma_{exh}-1}{\gamma_{exh}}} \left(1 + \frac{q_{in}}{c_v T_1 r_c^{\gamma_{exh}-1}}\right)^{\frac{1}{\gamma_{exh}}} \tag{4.12}$$

The specific energy of the charge per mass is:

$$q_{in} = \frac{W_{fuel} q_{HV}}{W_{eng_{In}} + W_{fuel}}(1 - x_r). \tag{4.13}$$

The residual gas fraction is:

$$x_r = \frac{1}{r_c}\left(\frac{p_{em}}{p_{im}}\right)^{\frac{1}{\gamma_{exh}}} \left(1 + \frac{q_{in}}{c_v T_1 r_c^{\gamma_{exh}-1}}\right)^{-\frac{1}{\gamma_{exh}}} \tag{4.14}$$

The model is complete with:

$$T_1 = x_r T_{em} + (1 - x_r)T_{im}. \tag{4.15}$$

In Matlab/Simulink, the non-linear equation system is solved in a fixed number of points and implemented using maps. This, because it is inefficient to solve the equations in real time.

4.1.4 Exhaust Manifold

The exhaust manifold is modelled as a control volume in the same way as the intake manifold (see section 4.1.2), that is by differentiating the ideal gas law. As for the intake manifold the temperature changes are assumed to be slow.

The flow into the exhaust manifold is the flow out of the engine and the flow out of exhaust manifold is the flow through the turbine.

$$W_{in} = W_{eng_{out}} \tag{4.16}$$

$$W_{out} = W_{trb} \tag{4.17}$$

Consequently, the derivative of the pressure in the exhaust manifold is given by 4.18, with V_{em} as the only parameter.

$$\dot{p}_{em} = \frac{R_{exh}T_{em}(W_{eng_{out}} - W_{trb})}{V_{em}} \tag{4.18}$$

4.1.5   Primary Turbine

As for the compressor (see section 4.1.1), the mass flow through and the torque produced by the turbine are of interest. To that, the temperature after the turbine is an input to other components in the model and hence needed as an output here. The torque equation is essentially the same as for the compressor, but for expanding instead of compressing the gas. The torque is given by:

$$\tau_{trb} = \frac{W_{trb}c_{p_{exh}}T_{em}\eta_{trb}}{\omega_{trb}} \left(1 - \left(\frac{p_{em}}{p_{es}}\right)^{\frac{1-\gamma_{exh}}{\gamma_{exh}}}\right) \tag{4.19}$$

As for the compressor, the mass flow and efficiency is modelled by maps provided by the manufacturer.

$$W_{trb} = f_{W_{trb}} \left(\frac{p_{em}}{p_{es}}, n_{trb}\right) \tag{4.20}$$

$$\eta_{trb} = f_{\eta_{trb}} \left(\frac{p_{em}}{p_{es}}, n_{trb}\right) \tag{4.21}$$

To this, the temperature after the turbine is modelled as:

$$T_{trb_{out}} = \left(1 + \eta_{trb}\left(\left(\frac{p_{em}}{p_{es}}\right)^{\frac{1-\gamma_{exh}}{\gamma_{exh}}} - 1\right)\right)T_{em} \tag{4.22}$$

4.1.6   Turbine Shaft

The turbine shaft connects the turbine and the compressor. By use of Newton´s second law the derivative of the turbine shaft speed can be modelled as:

$$\dot{\omega}_{trb} = \frac{1}{J_{trb}} \left(\tau_{trb} - \tau_{cmp}\right) \tag{4.23}$$

The same approach has previously been used in for example [5] and [11]. The parameter J_{trb} is estimated from measurement data.

4.1.7 Exhaust System

As above, the pressure is modelled using a standard control volume, assuming the temperature variations are slow. The flow into the volume equals the flow through the turbine and the flow out of the volume equals the flow through the exhaust pipe.

$$\dot{p}_{es} = \frac{R_{exh}T_{es}}{V_{es}}(W_{trb} - W_{es}) \tag{4.24}$$

The flow out of the volume is modelled using a quadratic restriction, with the restriction constant k_{es} [1]:

$$W_{es}^2 = \frac{p_{es}}{k_{es}R_{exh}T_{es}}(p_{es} - p_{amb}) \tag{4.25}$$

Here, the parameters k_{es} and V_{es} are estimated from measurement data.

4.2 Turbo Compound

The output signals of the turbo compound model is the flow through and the temperature after the compound turbine. The modelling of the turbine is similar to the primary turbine model (see section 4.1.1). Both the temperature submodel and the flow submodel take turbine speed and temperature before the turbine as input signals. As for the primary turbine, the temperature before the compound turbine is an output signal of the preceding component in the model, while the speed of the turbine shaft has to be modelled. The input and output signals are illustrated in figure 4.3.
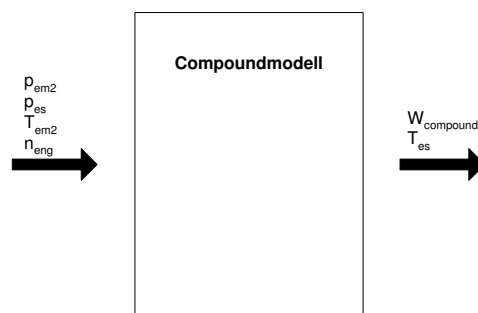

Figure 4.3: Input and output signals of the turbo compound model.

By studying the torques affecting the shaft, two main sources can be identified: the torque from the turbine and the torque transmitted in the hydraulic

coupling. This is not the complete picture, for example friction is neglected. The resulting torque on a rotating component is proportional to the derivative of the rotational speed by the factor $1/J$. The parameter J is the moment of inertia and is estimated from measurement data. Consequently the turbine speed can be calculated by integration of the resulting torque.

$$\dot{\omega} = \frac{1}{J}\tau \qquad\qquad (4.26)$$

The torque from the turbine is modelled in the same way as for the primary turbine (see section 4.1.5). The torque transmitted in the hydraulic coupling is determined by several factors, for example the slip, the speed of the coupling, the viscosity of the oil and the dimensions of the coupling. Lots of scientific articles have been produced on the topic of physical modelling of hydraulic couplings (see for example [14] [7]). After studying of literature and some testing, four models were selected for further evaluation:

- No slip model

- Föttinger-Kupplung

- Uniform velocity model

- Linear velocity model

4.2.1   No slip model

The hydraulic coupling is designed to have slip in the range -5 to 5 % [16] at the operating conditions in the vehicle. Consequently, a model that assumes that the turbine speed is the same as the geared engine speed has a maximum error of 5%. The mean error would be the mean of the absolute slip value. The no slip model, described by equation 4.27, is static and hence efficient for real time execution.

$$\omega = K n_{eng} \qquad\qquad (4.27)$$

4.2.2   Föttinger-Kupplung

Martyrer [9] presents a model for predicting the transmitted torque. Unfortunately, the physical background and derivation is not presented in the works we have managed to find. The original source [9] was searched for, but has not been found. Instead the equations have been taken from Föttinger-Kupplungen [7] and an internal Scania document [16]. The model predicts

the torque transmitted as:

$$\tau = K_1 S \rho \omega^2 D^5 = K S \omega^2 \text{ ,where}$$

$$
\begin{aligned}
K_1 &= \text{coupling specific constant} \\
S &= \frac{\omega_i - \omega_t}{\omega_i} \\
\rho &= \text{oil density} \\
\omega &= \text{angular velocity of turbine runner} \\
D &= \text{coupling specific diameter} \\
K &= \text{coupling specific constant}
\end{aligned}
\tag{4.28}
$$

Under the assumption that the density is constant over the operating temperature range, all the coupling specific constants, including the oil density, affects the torque proportionally, consequently they can be reduced to one single parameter, K. Hence, there is one parameter that has to be estimated from measurement data.

4.2.3 Uniform velocity model

The uniform velocity model is developed by Qualman and Egbert and is presented in [14]. The fluid flow in the coupling is considered to have two components: one circumferentially about the coupling axis and one flow from the impeller (driving coupling half) to the turbine. The model is a mean flow model, i.e. the flows are considered to follow only one single effective path in every dimension. Hence, there are two flow paths, one for the circumferentially flow and one for the flow between the coupling halves (see figure 4.4). Further, the velocity distribution is considered to be uniform (see figure 4.5)
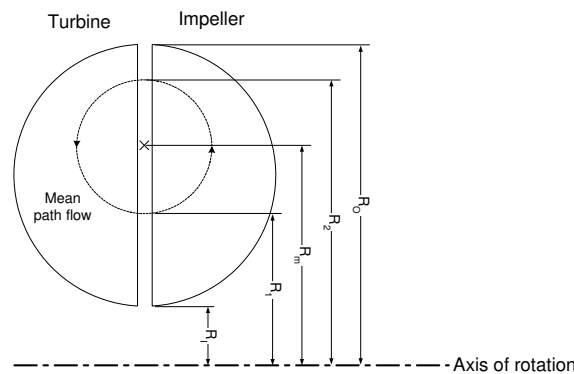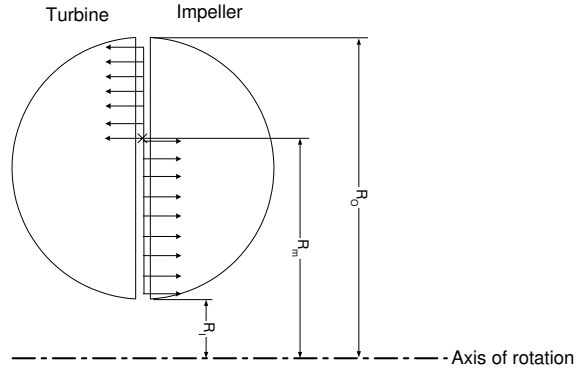

Figure 4.4: The mean flow path.

Figure 4.5: Uniform velocity flow model.

The center of the mean flow path is given by:

$$R_m = \sqrt{\frac{R_O^2 + R_I^2}{2}} \tag{4.29}$$

The mean radius of the upper flow (from the impeller to the turbine) and the lower flow (from the turbine to the impeller) is given by:

$$R_2 = \sqrt{\frac{R_O^2 + R_m^2}{2}} \tag{4.30}$$

$$R_1 = \sqrt{\frac{R_I^2 + R_m^2}{2}} \tag{4.31}$$

The torque developed is given by the rate of change of the angular momentum. The resulting angular momentum is the difference between the angular momentum of the upper and lower flows. Under the condition that the tangential velocity is the same as the velocity of the blade speed, the developed torque is given by:

$$\tau = \dot{m}(\omega_i R_2^2 - \omega_t R_1^2) \tag{4.32}$$

Further, the mass flow rate can be calculated:

$$\dot{m} = \rho\pi(R_m^2 - R_I^2)C \tag{4.33}$$

Thus, the only unknown parameter is the flow velocity, C, which can be evaluated by calculating the losses in the coupling.

The power is given by:

$$P = \omega\tau \tag{4.34}$$

Consequently, the input and output power is given by:

$$P_{in} = \dot{m}\omega_i(\omega_i R_2^2 - \omega_t R_1^2) \tag{4.35}$$

$$P_{out} = \dot{m}\omega_t(\omega_i R_2^2 - \omega_t R_1^2) \tag{4.36}$$

The losses are the difference between the input and the output power. Thus, the the power loss, expressed per unit of mass is:

$$P_{loss} = (\omega_i R_2^2 - \omega_t R_1^2)(\omega_i - \omega_t) \tag{4.37}$$

The losses are considered to consist of two parts: incidence losses and flow path circulation losses (friction). The incidence loss has two components, one originating from the pump side and one from the turbine side. The total incidence loss is:

$$P_{incidence\_loss} = \frac{1}{2}(R_2^2 + R_1^2)(\omega_i - \omega_t) \tag{4.38}$$

The flow path circulation losses is assumed to be proportional to the square of the flow between the pump and the turbine halves. Hence, the flow path circulation losses are given by:

$$P_{circulation\_loss} = \frac{1}{2}KC^2 \tag{4.39}$$

By equating (4.37) to the sum of the incidence loss, (4.38), and the circulation loss, (4.39), the circulation speed, C, can be derived with the loss coefficient, K, as the only parameter.

$$C = \sqrt{\frac{1}{K}\left(2\left(\omega_i - \omega_t\right)\left(\omega_i R_2^2 - \omega_t R_1^2\right) - \left(\omega_i - \omega_t\right)^2\left(R_1^2 + R_2^2\right)\right)} \tag{4.40}$$

Finally, the developed torque in the coupling can be calculated by use of (4.32).

$$\tau = \rho\pi C\left(R_m^2 - R_I^2\right)\left(\omega_i R_2^2 - \omega_t R_1^2\right) \tag{4.41}$$

4.2.4 Linear velocity model

On the basis of the uniform velocity model, Wallace has developed the linear velocity model. The main difference is that the assumption of uniform velocity has been changed to a linear velocity distribution originating from the center of the mean radius (see figure 4.6). Also, the expressions for incidence losses and circulation losses are calculated with the new velocity assumption and the circulation losses are divided into friction losses and other losses.
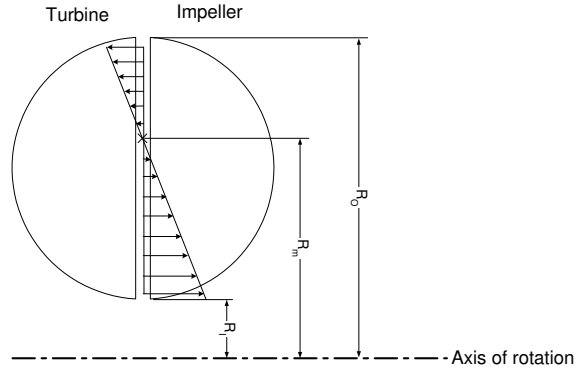
Figure 4.6: Linear velocity flow model.

Despite the changes above, the principle is similar. The massflow between the two coupling halves are calculated by equating two expressions of the total losses. The more detailed calculations of the losses leave one parameter to be estimated from measurement data.

The torque developed in the coupling is given by:

$$\tau = K_1 \omega_i \sqrt{\left(\frac{\omega_i^2 S \left(K_1 - S K_i \right)}{\mu} \right)}$$

$$K_1 = 2\pi\rho \left(\frac{R_O^5}{5} - \frac{R_O^4 R_m}{4} + \frac{R_m^5}{20} - (1 - S) \left(\frac{R_m^5}{20} - \frac{R_I^4 R_m}{4} + \frac{R_I^5}{5} \right) \right)$$

$$K_i = \pi\rho \left(\frac{R_m^5}{20} - \frac{R_I^4 R_m}{4} + \frac{R_I^5}{5} + \frac{R_O^5}{5} - \frac{R_O^4 R_m}{4} + \frac{R_m^5}{20} \right)$$

$\rho = $ oil density

$R_O = $ see figure 4.4

$R_I = $ see figure 4.4

$$R_m = \frac{2}{3} \frac{R_O^3 - R_I^3}{R_O^2 - R_I^2}$$

$\omega_i = $ angular velocity of impeller

$\omega_t = $ angular velocity of turbine

$$S = \frac{\omega_i - \omega_t}{\omega_i}$$

$\mu = $ loss parameter estimated from measurement data

(4.42)

The complete calculations for derivation of the model are far too extensive

to be presented in this thesis, for further reading article [14] can be studied.

4.3   Extended Model

In this section, the turbo compound model (see section 4.2) is integrated with the existing model (see section 4.1). The model is schematically depicted in figure 4.7.
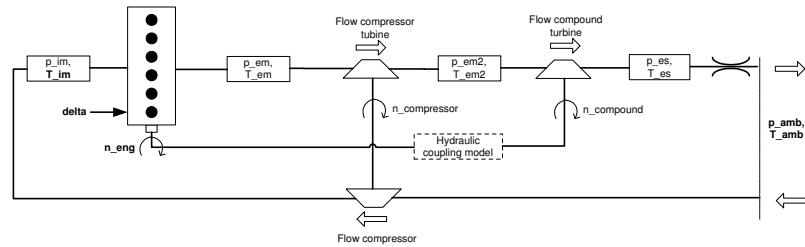

Figure 4.7: Extended model including turbo compound, input signals are bold.

The extended model will also contain another control volume, the pressure between the turbines. It is modelled in the same way as in the existing model, see section 4.1.2. The flow into the volume is the flow through the primary turbine, and the flow out is the flow through the compound turbine. The parameter estimated from measurement data is V_{em2} and the state equation is:

$$\dot{p}_{em2} = \frac{R_{exh}T_{em2}(W_{trb_1} - W_{trb_2})}{V_{em2}} \tag{4.43}$$

The input signals are the same for the extended model as for the existing model, see table 4.1. When it comes to output signals it is not that simple. There are lots of signals available in the models, that hence can be chosen as output signals. All of them have not been validated due to lack of appropriate measurement equipment. The signals that are validated (see chapter 6) are also seen as output signals, see table 4.2. Consequently, another measurement setup would have lead to other output signals. Hence, other signals are potential output signals, for example the torque transmitted from the turbo compound to the crankshaft, different temperatures and mass flows in the engine.

4.4   Modularity

Modularity means that submodels can be changed or substituted, without affecting the rest of the model in terms of input and output signals. This is

Table 4.1: Input signals

Signal	Description
p_{amb}	Ambient pressure
T_{im}	Inlet manifold temperature
T_{amb}	Ambient temperature
n_{eng}	Engine revolution speed
δ	Injected fuel

Table 4.2: Output signals

Signal	Description
p_{im}	Intake manifold pressure
p_{em}	Exhaust manifold pressure
p_{em2}	Pressure between the turbines
p_{es}	Exhaust system pressure
n_{trb}	Primary turbine speed
n_{trb2}	Compound turbine speed

closely connected with the implementation of the model. Each submodel is implemented as a separate component in Matlab/Simulink, which makes the implementation modular.

Besides that the modularity makes it easy to change or substitute the submodels, there are other advantages as well. For example, it makes it easier for people not directly involved in the model development to understand the structure and hence to contribute to it or take over the work. This is an important issue in industrial applications.

A condition for the modular implementation is that the equations that are implemented have a suitable structure. Thus, there has to be separate equations for each component constituting a submodel. In physical modelling this is natural, but when using blackbox models this has to be thought of. In this thesis, all models are physically based and hence the equations are easy to implement in a modular way.

Chapter 5

Calibration

In this chapter, the calibration approach used in this thesis will be described. Before this work, all parameters were tuned manually by "trial and error" on the complete engine model. The manual calibration has several disadvantages. One is that it requires that the person doing the tuning has good knowledge of the model and an understanding of how the parameters affect the outputs. The manual tuning is also a time consuming process. By having a systematic way of setting the parameters, these disadvantages can be reduced. Automatization would also help to lessen these disadvantages.

In the modularity perspective, it is not desirable to set the parameters on the complete model. This would mean that if one component in the model was changed, the complete calibration process must repeated.

5.1 Optimization

By using optimization to set the parameters, the systematics is increased. This is because how to change the parameters to achieve better model performance is decided by the optimization procedure. And since the change of parameters is clearly determined, the process can easily be automatized by an iterative approach. Lars Eriksson has developed the `lsoptim` package, which is a least-square optimization program. It solves non-linear unconstrained optimization problems. By taking small steps in the parameter vector and analyzing the residual, an approximation of the hessian is achieved. From the hessian estimated, the new parameter vector is calculated by a variant of the Levenberg-Marquardt method. For more details on the algorithm, see *Minimal manual to* `lsoptim` [4].

The `lsoptim` package works well, and usually finds the optimum after few iterations. However, some problems occurred. One is that it finds local optima, which means that the initial values are important. They must be manually chosen in a good way, and hence some of the automatization is lost.

Another problem was that when there were many parameters, it was difficult to find the optimum. When optimizing physical parameters such as volumes, they were sometimes given negative values, which is not realistic. In these cases, the parameters were adjusted manually.

5.2   Systematics and Modularity

To achieve high modularity, the calibration was done by optimizing as small subsystems as possible. The subsystems were then put together to a complete engine model. When calibrating the subsystems, all input signals were measured signals or control signals from S6. However, since the temperature measurement in the vehicle was bad and the mass flow was not possible to measure these input signals came from simulation. Consequently, the performance of one subsystem will affect the calibration of the subsystems using input signals from it, and hence the modularity is reduced.

The calibration strategy described above gave results quite up to the standard of the existing model, but an analysis showed that the errors were mainly caused by a bad accuracy of the turbine speed. Therefore, an optimization of the correction parameters for the efficiency of the primary turbine and the compressor, were made on the complete engine model. This is not good in terms of modularity, but it increased the accuracy enough to be valued higher than the loss of modularity.

When setting the parameters, all physical constants were given their correct values. Also, the volumetric efficiency was not optimized, but taken from engine test bed measurements. The parameters optimized were volumes, moments of inertia and a restriction constant. It also turned out that the flows through and efficiencies of the compressor and the turbines were not correct, and therefore correction maps were added to the original maps. These correction maps were also optimized. For more details and discussion on the performance and validity of the compressor and turbine maps, see section 6.2.8.

The data used for optimization was dynamic data from measurements in a vehicle. To get good model performance, data covering the complete operating range is needed. During the optimization the problem with fitting the parameters to tight to certain data was encountered. The problem was not mainly that noise affected the optimization, but that the data was not representative for all driving conditions. For example, if the parameters were optimized with data from high way driving, the performance was bad when validating on city driving data. A combination of city driving and high way driving turned out to give data varying enough, and was used for optimization. Table 5.2 shows the optimization steps of the extended model, when the turbo compound was modelled using the Föttinger-Kupplung model.

Table 5.1: Optimization steps

Step	Optimized quantity	Optimized parameters	Manually adjusted parameters
1	Intake manifold pressure	Flow correction map for compressor	Intake manifold volume
2	Exhaust manifold pressure	Flow correction map for turbine 1, exhaust manifold 1 volume	
3	Pressure between the turbines	Flow correction map for turbine 2, exhaust manifold 2 volume	
4	Compound turbine speed	Efficiency correction map for turbine 2, moment of inertia for turbine shaft 2, coupling parameter	
5	Exhaust system pressure	Restriction constant, exhaust system volume	
6	Primary turbine speed	Efficiency correction maps for compressor and turbine 1, moment of inertia for turbine shaft 1	

Chapter 6

Validation

In this chapter, the models are validated using dynamic data collected in a vehicle. First the different turbo compound submodels are validated and the results are evaluated. Further, the submodels to be integrated with the existing model for further evaluation are chosen. The extended models are then validated and the result is compared to the existing model. For all validation, data different from the one used for calibration is used.

Error is measured by the measures mean error, root mean square error and maximal error. Also, the distribution of the error is analyzed using histogram plots.

$$\text{mean relative error} \quad = \quad \frac{1}{n} \sum_{i=1}^{n} \frac{|\hat{x}(t_i) - x(t_i)|}{|x(t_i)|} \qquad (6.1)$$

$$\text{root mean square error} \quad = \quad \sqrt{\frac{1}{n} \sum_{i=1}^{n} \left(\frac{\hat{x}(t_i) - x(t_i)}{x(t_i)} \right)^2} \qquad (6.2)$$

$$\text{maximum relative error} \quad = \quad \max_{1 \le i \le n} \frac{|\hat{x}(t_i) - x(t_i)|}{|x(t_i)|}, \qquad (6.3)$$

where $x(t_i)$ is the measured quantity, $\hat{x}(t_i)$ is the simulated quantity and n is the number of samples.

The signals validated are decided by what signals that are possible to measure with sufficient accuracy, that is the pressures and the turbine speeds. The flows and temperatures could not be measured with sufficient accuracy (see section 3.3), hence they are not validated. However, some observations regarding the exhaust gas temperature model was done.

All simulations were done using discrete components and fixed step length of 10 milliseconds. The step length is chosen to be the same as the step length used in S6. Also, step length sensitivity tests are made, where the discrete

fixed step length simulations are compared to continuous variable step length simulations.

Three kinds of driving conditions are used: city driving, high way driving and mixed driving.

City driving Many stops and accelerations, speeds up to 60 km/h.

High way driving Few accelerations and retardations, speeds from 70 to 90 km/h.

Mixed driving Includes both city and high way driving, and also parts on smaller roads with speeds in the range 40 to 70 km/h.

All data collection is done in the areas around Södertälje, which means that there are restrictions on for example hill length, level over the sea and temperatures.

6.1 Turbo Compound

For the turbo compound models, the validated signal is the turbine speed. The models were simulated with measured pressures before and after the compound turbine and engine speed from S6. Due to bad temperature measurement, simulated temperature from the preceding components were used. First, the different models tested are evaluated by them selves and then the results are compared.

6.1.1 No slip model

The no slip model is static, hence, the simulation stability is not dependent of step length. The errors are presented in table 6.1. The histogram of the relative error, and consequently the slip, for mixed driving (see figure 6.1) shows that slips around 0 and 5 % are the most common. The distribution of the slip is similar for the city and high way driving. Hence, it would have been good if the model had captured the behaviour in those particular areas. This is the case for zero-slip, but as the error equals the slip, this is not the case for the 5% area. Even though it is hard to see in the figure, there are short periods of time, where the slip is greater than the $\pm 5\%$ stated in section 4.2. This occur in some gear shifts, but the slip is very fast brought back to the the $\pm 5\%$ area.

Consequently, the model is good at low load condition and worse at high load condition. In some gear shifts the error is up to 11.5%, but is else in the $\pm 5\%$ area. The fact that the model is static and simple (no non-linear terms), makes it suitable for real time execution.

Table 6.1: No slip model validation

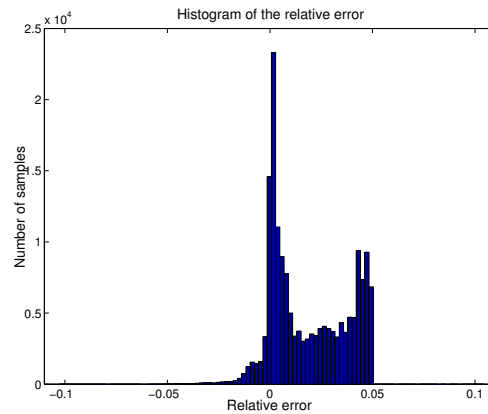| Driving condition	Rel. error (%)		
	mean	rms	max
City driving	1.25	1.76	5.72
Highway driving	1.83	2.60	4.91
Mixed driving	2.02	2.70	11.5

Figure 6.1: Histogram of the relative errors for the no slip model, mixed driving.

6.1.2 Föttinger-Kupplung

The mean and rms errors for all driving conditions are very low (see table 6.2). For mixed driving the maximum error is much larger than for the other driving conditions. Still, the relative error histogram (see figure 6.2) shows that errors around the maximum error occur for very small periods of time. The error distribution is approximately gaussian and fairly symmetric around zero. Hence, it can be assumed that most of the system behaviour is described and that the error can be related to noise. The performance of the model is very good, with some occasional problems for the mixed driving condition.

An analysis of the step length sensitivity was also done and it shows that a step length of approximately 50 milliseconds can be used without stability problems.

6.1.3 Uniform velocity distribution

The performance of the model almost as good as for the Föttinger-Kupplung model (see table 6.3), and superior to the no slip model. All errors, but the mean error for city driving, are larger than for the Föttinger-Kupplung

Table 6.2: Föttinger-Kupplung model validation

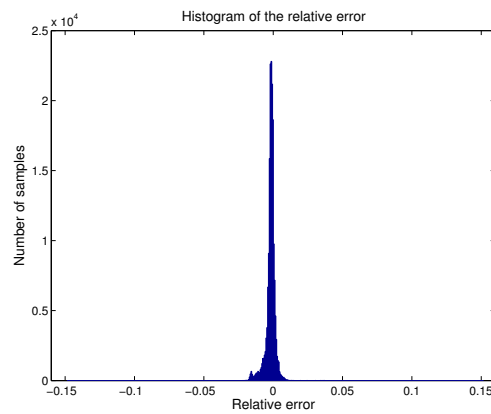| Driving condition	Rel. error (%)		
	mean	rms	max
City driving	0.419	0.556	5.00
Highway driving	0.235	0.264	1.40
Mixed driving	0.260	0.462	15.1

Figure 6.2: Histogram of the relative errors for the Föttinger-Kupplung model, mixed driving.

model. The error distribution plot (see figure 6.3) is approximately gaussian, but is slightly displaced to the left. This indicates that there are some system behaviour that is not modelled. Despite the small displacement and slightly larger errors than the Föttinger-Kupplung model, the model performance must be considered as very good.

The step-length sensibility-test shows that the model has some oscillative tendencies at 50 milliseconds (see figure 6.4), but the error is still acceptable.

Table 6.3: Uniform velocity distribution model validation

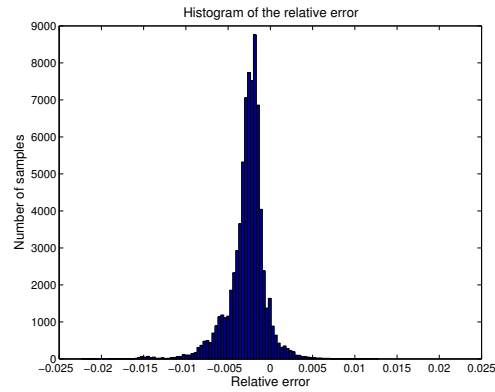| Driving condition	Rel. error (%)		
	mean	rms	max
City driving	0.400	0.584	7.58
Highway driving	0.291	0.355	2.24
Mixed driving	0.352	0.759	38.2

Figure 6.3: Histogram of the relative errors for the uniform velocity distribution model, high way driving.
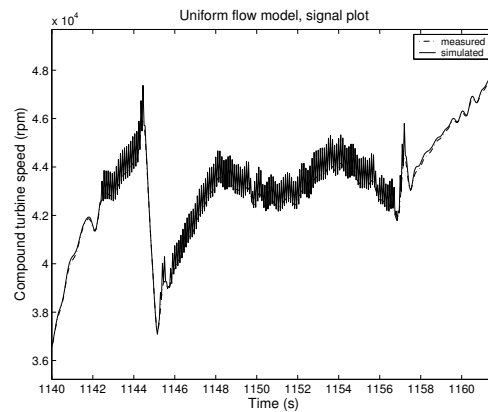

Figure 6.4: Oscillations of the compound turbine speed simulated with the uniform velocity distribution model at fixed step length of 50 milliseconds.

6.1.4   Linear velocity distribution

The performance of the linear velocity distribution model is much worse than all the other models (see table 6.4). All errors measured are larger than for the other models and oscillative tendencies can be seen already at the step length of 10 milliseconds (see figure 6.5).

It may seem strange that a model, which is a development of a high performance model, show worse result than the original model. Due to the high performance of the models already tested, this has not been investigated further.

Table 6.4: Linear velocity distribution model validation

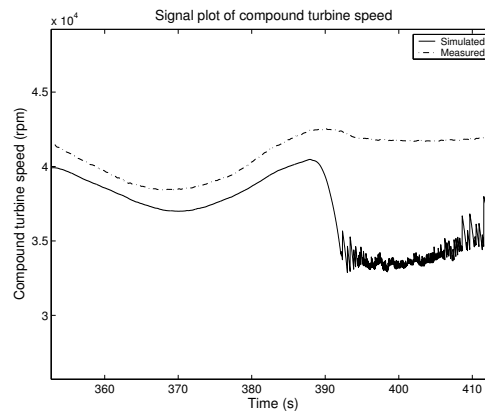| Driving condition	Rel. error (%)		
	mean	rms	max
City driving	12.8	16.3	66.7
Highway driving	12.6	16.9	37.7
Mixed driving	12.4	16.3	83.5

Figure 6.5: Signal plot of linear velocity distribution model showing oscillations.

6.1.5 Summary

Two models have been chosen for further evaluation by integration with the existing model: the no slip model and the Föttinger-Kupplung model.

All models tested are physical and must be considered equivalent in terms of modularity. This, because all turbo compound models can be substituted with each other in the extended engine model, without that changes have to be made in the rest of the model. According to the criteria stated in the objectives (see section 1.3), there are two criteria left for separating the models: accuracy and real time execution ability.

The accuracy is measured by the mean, rms and maximum errors presented for each model. For the ability of real time execution, it is not that simple. Several qualities are desired for models that are to be executed in real time, for example execution using fixed step length, low demand for computer power and low memory demand. In this thesis, the static model is considered as demanding less computer power than the state models. Longer step length is, thereto, considered as contributing to better real time execution ability.

Due to much worse accuracy than the other models, the linear velocity distribution model can immediately be excluded from further evaluation. The model is, thereto, the most complicated and shows bad step length perfor-

mance. The remaining models have errors small enough to be interesting for further evaluation.

The no slip model is superior to the other models in terms of real time execution ability, this because it is static. Hence, the no slip model, with fair accuracy and excellent real time execution ability, is chosen for further evaluation.

The Föttinger-Kupplung model is slightly better than the uniform velocity distribution model, both in terms of accuracy and real time execution ability. Thus, it is not likely that the uniform velocity distribution model would improve the overall performance of the extended model. Hence, the Föttinger-Kupplung model and the no slip model is picked for further evaluation.

6.2   Extended model

In this section, the turbo compound submodels chosen above are integrated with the existing model. The signals validated are four pressures (intake manifold, exhaust manifold, between the turbines and in the exhaust system) and two turbine speeds (primary turbine and compound turbine). Validation of the extended model with both the turbo compound models chosen in section 6.1.5 is made.

6.2.1   Intake Manifold Pressure

For both implementations of the turbo compound model, the errors are very similar. Hence, the accuracy difference of the turbo compound model does not effect the intake manifold pressure significantly. The mean and rms errors must be considered as very small, but the maximum errors are quite large (see table 6.5). Figure 6.6 shows a histogram of the relative error, which is approximately gaussian and symmetric around zero. Hence, it indicates that there are no systematic errors. The histogram presented is for the Föttinger-Kupplung model and mixed driving conditions, but the shape is similar for the other cases.

Almost always, the simulated intake manifold pressure is smooth and follows the measured signal very well. Figure 6.7 shows the typical behaviour. Occasionally, at low pressures, the signal becomes oscillative (see figure 6.8). The amplitude of the oscillations is moderate, and there are no stability problems. The problem has earlier been observed for the existing model. No further investigation of the causes has been made.

6.2.2   Exhaust Manifold Pressure

As for the intake manifold pressure, the difference between the two turbo compound models is insignificant. In both cases the mean and rms errors are small, but the maximum error is much larger (see table 6.6).

Table 6.5: Intake manifold pressure validation

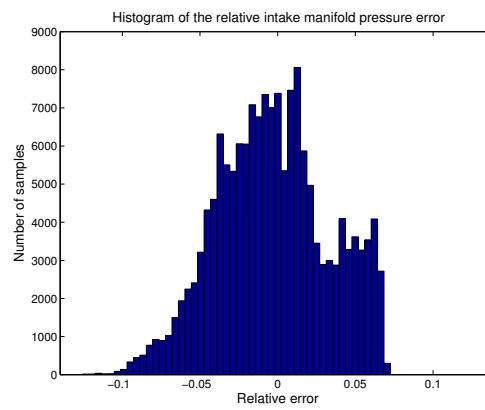| Driving condition | Relative error (%) | | | | | |
| | No slip | | | Föttinger-Kupplung | | |
	mean	rms	max	mean	rms	max
City driving	3.38	4.60	20.5	3.34	4.55	20.6
Highway driving	2.06	2.78	10.5	1.97	2.66	10.5
Mixed driving	2.95	3.62	13.4	2.94	3.62	13.3

Figure 6.6: Histogram of the relative error distribution of the intake manifold pressure, mixed driving condition.
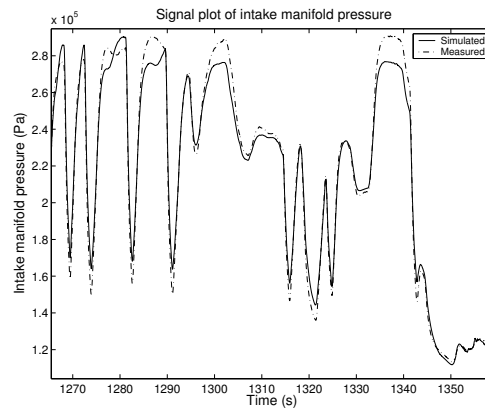

Figure 6.7: Typical signal plot of the intake manifold pressure.

The relative error distribution, presented in figure 6.9, is displaced approximately 2 percent units to the right, which indicates that there are some
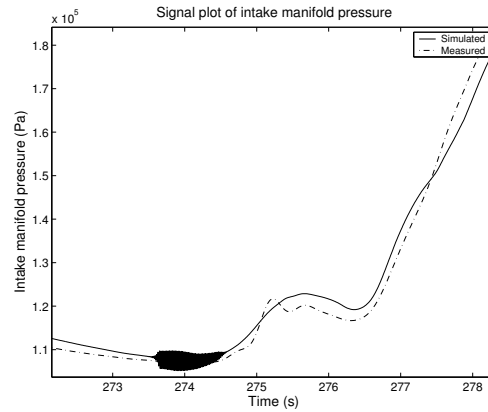
Figure 6.8: Oscillations of the intake manifold pressure.

systematic error. This may be due to the model structure, but can also be a calibration problem.

Table 6.6: Exhaust manifold pressure validation

| Driving condition | Relative error (%) | | | | | |
| | No slip | | | Föttinger-Kupplung | | |
	mean	rms	max	mean	rms	max
City driving	2.26	3.10	12.9	2.51	3.07	12.9
Highway driving	2.32	2.74	9.03	2.27	2.67	9.04
Mixed driving	2.72	3.78	33.2	2.76	3.79	33.1

6.2.3 Pressure Between the Turbines

As for the other pressures, the accuracy of the pressure between the turbines is very good for both turbo compound models. The errors are presented in table 6.7. Compared to the intake and exhaust manifold pressures, all errors measured are lower. The error distribution (see figure 6.10) is displaced to the right and is similar for both turbo compound models and all driving conditions. Hence, the model structure may have systematic errors or the optimal parameters have not been found in the calibration procedure.

6.2.4 Exhaust System Pressure

The exhaust pressure has the smallest relative errors of all pressures, still, the model seems to have systematic errors (see figure 6.11). Figure 6.12 shows a
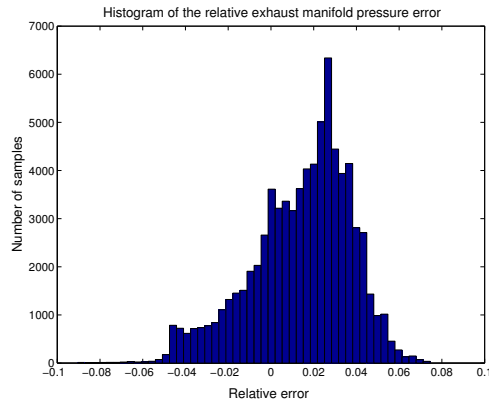
Figure 6.9: Histogram of the relative error distribution of the exhaust manifold pressure, highway driving condition.

Table 6.7: Validation of pressure between the turbines

Driving condition	Relative error (%)					
	No slip			Föttinger-Kupplung		
	mean	rms	max	mean	rms	max
City driving	1.36	1.73	9.61	1.35	1.74	10.1
Highway driving	1.85	2.18	5.66	1.90	2.21	6.25
Mixed driving	2.23	1.99	26.5	2.36	3.51	24.8

Figure 6.10: Histogram of the relative error distribution of the pressure between the turbines, highway driving condition.

signal plot of the exhaust system pressure and clarifies that the model is not optimal.

Table 6.8: Exhaust system pressure validation

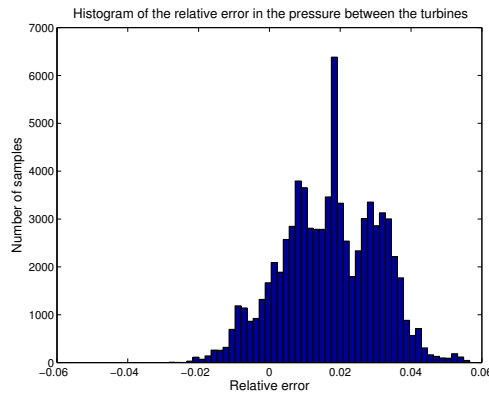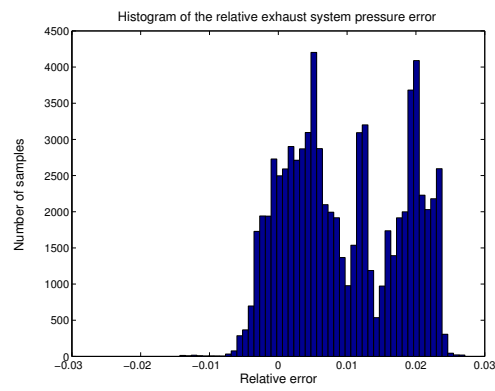| Driving condition | Relative error (%) | | | | | |
| | No slip | | | Föttinger-Kupplung | | |
	mean	rms	max	mean	rms	max
City driving	0.877	0.993	2.32	1.01	1.10	3.01
Highway driving	1.02	1.28	2.71	1.36	1.51	3.60
Mixed driving	0.913	0.896	2.96	1.28	1.39	3.44

Figure 6.11: Histogram of the relative error distribution of the exhaust system pressure, highway driving condition.
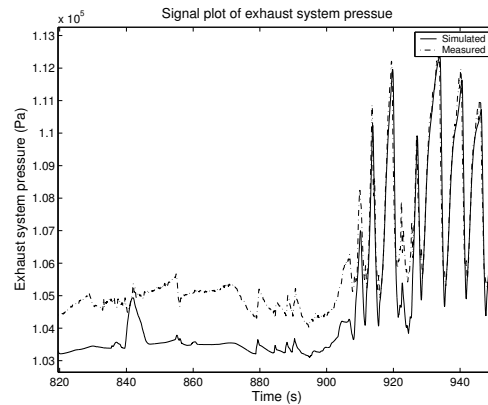

Figure 6.12: Typical signal plot of the exhaust system pressure.

6.2.5   Primary Turbine Speed

As for the other quantities validated above, the accuracy of the primary turbine speed is almost equivalent for the two turbo compound models. The mean and rms errors are fairly low, but the maximum error is quite large (see table 6.9).

The error distribution is approximately gaussian and centered around zero for the highway driving conditions but, for the other two conditions there are displacement to the left. An example of the error distribution is presented in figure 6.13. Thus, there are some systematic error in the model.

Table 6.9: Primary turbine speed validation

Driving condition	Relative error (%)					
	No slip			Föttinger-Kupplung		
	mean	rms	max	mean	rms	max
City driving	5.24	8.12	33.5	5.13	7.98	33.3
Highway driving	2.06	2.80	11.6	2.08	2.84	11.6
Mixed driving	3.40	5.27	31.8	3.42	5.25	31.4
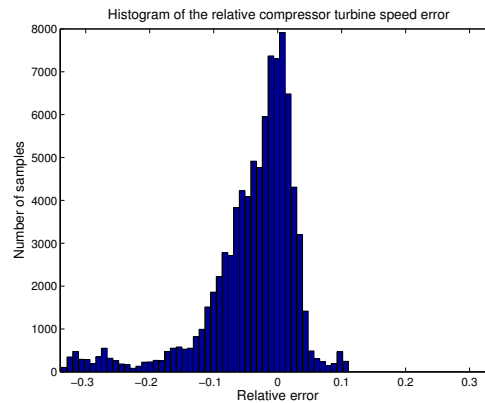
Figure 6.13: Histogram of the relative error distribution of the primary turbine speed, city driving condition.

6.2.6   Compound Turbine Speed

The extended model with the Föttinger-Kupplung turbo compound model shows better accuracy than the extended model with the no slip model. The relation between the errors of the two models is approximately the same as when the models were validated by them selves. For the no slip model, the error equals the slip and consequently the errors are exactly the same as in

section 6.1.1. For the Föttinger-Kupplung model, the errors are, on average, slightly larger than when it is validated using measured signals. This is natural, as the model is calibrated using measured data and the signals in the model deviates from the measured.

The error distributions are similar to the ones presented in section 6.1.2. A systematic error for the no slip model can, as expected, be seen in figure 6.1. For the Föttinger-Kupplung model, the distribution is approximately gaussian and symmetric around zero (see figure 6.2).

Table 6.10: Compound turbine speed validation

| Driving condition | Relative error (%) | | | | | |
| | No slip | | | Föttinger-Kupplung | | |
	mean	rms	max	mean	rms	max
City driving	1.25	1.76	5.72	0.582	0.796	5.51
Highway driving	1.83	2.60	4.91	0.224	0.280	1.48
Mixed driving	2.02	2.70	11.5	0.321	0.580	21.6

6.2.7 Exhaust Gas Temperature Observations

Even though the temperature measurements are bad (see section 3.2.2), some observations can still be made. In figure 6.14, the simulated and measured exhaust gas temperature are shown. The slow dynamics of the temperature sensor is clearly seen. It is also interesting to notice that the highest simulated temperature is lower than the highest measured temperature. At high temperatures, the radiation and heat conduction from the pipe walls will cool the thermoelement and thus give too low measured temperature. Hence, the simulated temperature should be higher than the measured. Since it is not, the simulated temperature is clearly too low.

The exhaust gas temperature model also assumes that there is no heating of the gas when no fuel is injected. It is reasonable to think that there still is some heating, for example radiation from the engine block.

6.2.8 Summary

The accuracy of the pressures and the primary turbine speed seem to be insensitive to errors in the compound turbine speed, at least when the errors are as small as for the models tested. Hence, the accuracy of the quantities, other than compound turbine speed, is almost independent of which of the turbo compound model that is used. In terms of step length sensitivity, both the extended models have approximately the same performance, see figure 6.15. However, the no slip model is linear and static, and is hence considered to demand less computational power than the nonlinear dynamic Föttinger-Kupplung model.
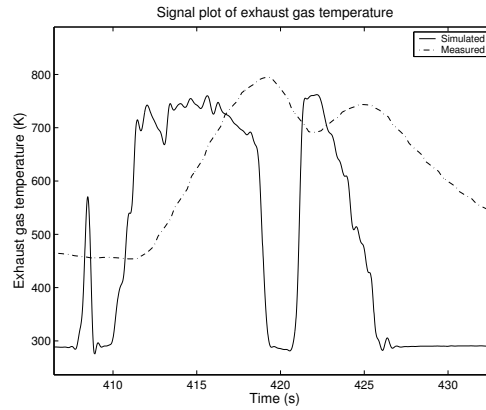
Signal plot of exhaust gas temperature

Figure 6.14: Signal plot of the exhaust gas temperature showing the too low simulated temperature.

Step length sensibility of the extended models
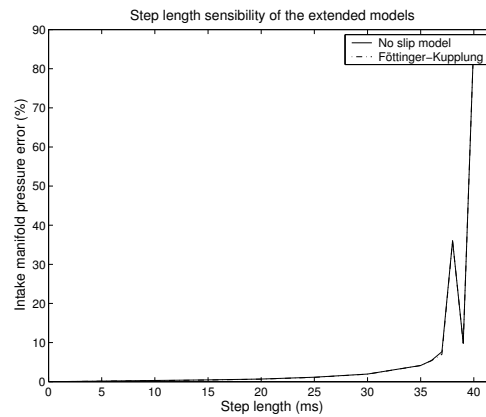
Figure 6.15: Error as a function of step length for the extended models.

The different extended models are consequently very similar in both accuracy and real time execution ability, which makes the choice difficult. If the compound turbine speed is an important output signal, the Föttinger-Kupplung is superior, if computational power is important, the no slip model is probably the best choice. Else, the performance must be considered as approximately equivalent.

Some of the submodels of the existing model have systematic errors, and it may be possible to get better performance if either the model structure is changed or the parameters is fitted in a better way. This may be because the parameters were only optimized using measured signals and as few submodels as possible (see chapter 5), which might lead to worse performance.

Probably, optimization of the complete extended model would give even better performance. This, because the parameters for each submodel can help to compensate for errors in other submodels.

Compared to the existing model, the accuracy of the extended models are good. In table 6.11, the intake manifold errors for the existing model and the best extended model is presented as an example. The mean errors for the pressures are in general lowered, with the intake manifold pressure and exhaust system pressure as the pressures improved the most. All errors except the maximum error for the exhaust manifold pressure during mixed driving are lowered. The quantity most improved is the primary turbine speed, where the mean errors are lowered by at least a factor three and the maximum errors are halved. This, despite that more complexity in form of the turbo compound and one more control volume is added. The excellent accuracy of the compound turbine speed model and the method for setting the parameters are probably the main reasons for the achieved accuracy. Thereto, the quantities added show comparable or better accuracy.

Table 6.11: Intake manifold pressure comparison

	Relative error (%)			
Driving condition	Existing model		Extended model	
	mean	max	mean	max
City driving	4.9	30.8	3.34	20.6
Highway driving	3.4	12.8	1.97	10.5
Mixed driving	5.8	25.2	2.94	13.3

Also, the step length sensitivity is better than for the existing model. The extended models have stability problems at step lengths from approximately 35 milliseconds, while the existing model got unstable at approximately 15 milliseconds. By adding complexity to the model, the real time stability has thus increased. During the implementation, it has shown that the real time execution ability depends on how the equations are implemented. Accordingly, either the extension of the model with turbo compound has a stabilizing effect or the implementation is better in terms of real time execution ability. An interesting area for further work is to investigate how the implementation affects the step length sensitivity.

As presented above, the accuracy of the extended models are very good in terms of the signals validated. Still, there are a lot of questions left. The temperature, torque and flow models are not validated at all, consequently, the accuracy of these signal are unknown. The area of use for the model would probably increase if these signals could be modelled with high accuracy. Consequently, this is an interesting area for further investigations.

The accuracy is remarkable, considered that the exhaust gas temperature model, even though it is not validated correctly, seems quite bad (see section 6.2.7). Probably, this has been compensated in the calibration, especially in

correction of the efficiency and flow maps. The corrections of the maps are quite large in some areas, which might be because of the incorrect temperature input signals. Due to bad temperature measurements, the maps have not been tested with correct input signals. With better input signals, it is possible that only small corrections of the maps are needed. Hence, the initial values of the optimization would be easier to find and consequently, the calibration procedure would be simpler.

Chapter 7

Conclusions and Future Work

Four models of the turbo compound have been tested. Two models were picked for integration with the existing model; the no slip model and the Föttinger-Kupplung. The Föttinger-Kupplung model has the best accuracy and has mean turbine speed errors lower than 1 % for all driving conditions. The error of the no slip model equals the slip in every point of time, the mean absolute slip, and hence the mean error, is about 2 %.

By integration of the turbo compound models with the existing model forming a complete mean value engine model, the difference in accuracy showed to be insignificant for all magnitudes except the compound turbine speed. For this magnitude, the errors were approximately the same as when the turbo compound submodels were validated using measured signals as inputs.

In real time execution ability, there was a slight advantage for the no slip model implementation. Both the extended models could execute with approximately the same step length (35 milliseconds) without stability problems, but the no slip model is static and hence considered as better in terms of real time execution ability. The choice is hence dependent on if the real time execution ability is critical or if accuracy of the compound turbine speed is important.

The extended models are superior to the existing model in terms of both accuracy and step length sensitivity. All pressures have lower mean errors than the existing model. For example, the mean error of the intake manifold pressure for mixed driving is lowered from 5.8 % to about 3.0 %. All maximum errors, but the exhaust manifold pressure at mixed driving condition, are also lowered.

The exhaust gas temperature has, without proper validation, shown to be inaccurate. It is remarkable that the accuracy of the extended models are as good as presented above, even though the exhaust gas temperature model is

not accurate. Probably, this is compensated by quite large corrections of the efficiency and flow maps of the turbines and compressor.

Both extended models are modulary implemented, i.e. each submodel could easily be substituted or added without changing the rest of the model. A systematic calibration approach has also been used. First, as small submodels as possible are calibrated using measurement data. The submodels are then put together. The procedure worked well, except for the primary turbine speed that had to be optimized together with the complete engine model. During the calibration, an optimization package, `lsoptim`, was used. This is an improvement from the previous calibration procedure, where the parameters were tuned manually.

7.1   Future Work

During the work with this thesis a couple of interesting areas for further investigations have come up. In this section some of them are presented.

As presented several times in the thesis, there have been problem with measuring the exhaust gas temperature. This caused severe validation problems, since no temperature model could be validated. A faster and more accurate (for example shielded from radiation) measurement is a necessary condition for further development of temperature models for dynamic conditions. Consequently, better temperature measurements are very important to improve the existing temperature models and hence the complete engine model.

Even though no proper validation has been made, the model of the exhaust gas temperature has shown systematic error. Due to bad temperature measurement, the effect on the rest of the model has not been investigated. Still, the large corrections of the turbine maps is a sign of that something is wrong. Incorrect exhaust gas temperature is one possible cause. It would hence be interesting to find a more accurate exhaust gas temperature model.

In this thesis a systematic and partly automatic calibration procedure has been used, which has made the procedure much easier and, to that, increased the accuracy. Still, the optimization is sensitive to what initial values that are used and there were occasionally problems with physically positive values getting negative. Solutions to these problems would improve the calibration procedure even more, thereto, a systematic way of detecting the global optimum would be beneficial.

If the turbine and compressor maps, with correct temperatures, turn out to be as bad as they are now, the optimization procedure would benefit of a more sophisticated interpolation function. Now, linear interpolation is used for the rectangular correction maps used in the optimization, which gives constraints on where to place the correction values. The rectangular shape is not optimal, since only a small part of the map is used. Points far from the area used can hence be given unrealistic values during optimization, which makes the

model sensitive to what map area used for optimization.

One way of measuring the errors during validation is, as in this thesis, to use mean, rms and maximum error. Together with the error distribution, this tells a lot about the quality of the model. Still, the measures are quite general and is not adapted to a special application. The generality can be seen as a strength, as well as a weakness. It would be interesting to look further into more application specific validation procedures, for example for diagnosis purposes.

References

[1] J. Biteus. MVEM of DC12 scania engine. Technical report, Department of Electrical Engineering, Linköping University, May 2002.

[2] O. Edfast, P. Floberg, C. Edelsvärd, and S. Nilsson. Temperaturgivare vid c-lab. Internal Scania document.

[3] D. Elfvik. Modelling of a diesel engine with vgt for control design simulations. Master's thesis IR-RT-EX-0216, Department of Signals, Sensors and Systems, Royal Institute of Technology, Stockholm, Sweden, July 2002.

[4] L. Eriksson. *A Minimal Manual to lsoptim*. Department of Electrical Engineering, Linköpings Universitet.

[5] L. Guzzela and A.Amstutz. Control of diesel engines. *IEEE Control Systems*, AC-37(7):53–71, October 1998.

[6] J. B. Heywood. *Internal Combustion Engine Fundamentals*. McGrae-Hill, 1988.

[7] E. Kickbusch. *Föttinger-Kupplungen und Föttinger-Getriebe*. Springer-Verlag, 1963.

[8] Kistler Instrumente AG. *Piezo instrumentation, Piezoresistive Absolute Pressure Sensors*, November 1998.

[9] E. Martyrer. Neure untersuchungen an föttinger-kupplungen, 1958.

[10] L. Nielsen and L. Eriksson. Course material, vehicular systems. Department of Electrical Engineering, Linköping University, 2002.

[11] S. Öberg. Identification and improvements of an automotive diesel engine model purposed for model based diagnosis. Master's thesis LiTH-ISY-EX-3161, Department of Electrical Engineering, Linköping University, Linköping, Sweden, December 2001.

[12] J. Ritzén. Modelling and fixed step simulation of a turbo charged diesel engine. Master's thesis LiTH-ISY-EX-3442, Department of Electrical Engineering, Linköping University, Linköping, Sweden, June 2003.

[13] P. Skogtjärn. Modelling of the exhaust gas temperature for diesel engines. Master's thesis LiTH-ISY-EX-3378, Department of Electrical Engineering, Linköping University, Linköping, Sweden, December 2002.

[14] F.J. Wallace, A. Whitfield, and R. Sivalingam. A theoretical model for the performance prediction of fully filled fluid couplings. *International Journal of Mechanical Science*, 20:335–347, 1978.

[15] F. Westin. Accuracy of turbocharged si-engine simulations. Technical report, Internal Combustion Engines Department of Machine Design, Royal Institue of Technology, Stockholm, Sweden, 2002. Licentiate thesis.

[16] H. Wikström. Prov med gummikoppling och hydraulkoppling för turbocompoundmotor. Internal Scania document, 1989.

Notation

Table 7.1: Symbols used in the report.

Symbol	Value	Description	Unit
c_p	Con	Specific heat capacity at constant pressure	$J/(kg \cdot K)$
c_v	Con	Specific heat capacity at constant volume	$J/(kg \cdot K)$
γ	Con	Ratio of heat capacities, c_p/c_v	$-$
δ	Var	Amount of injected fuel	$kg/stroke$
η	Var	Efficiency	$-$
η_{vol}	Var	Volumetric efficiency	$-$
R	Con	Gas constant, $c_p - c_v$	$J/(kg \cdot K)$
τ	Var	Torque	Nm
n	Var	Rotational speed	rpm
ω	Var	Rotational speed	$\frac{1}{s}$
N_{cyl}	Con	Number of cylinders	$-$
p	Var	Pressure	Pa
$\dot{p}$	Var	Derivative of pressure	Pa/s
q_{HV}	Con	Heating value	J/kg
T	Var	Temperature	K
V	Con	Volume	m^3
W	Var	Mass-flow	kg/s
$\dot{m}$	Var	Mass-flow	kg/s
x_r	Var	Residual gas fraction	$-$
r_c	Con	Compression ratio	$-$
J	Con	Moment of inertia	Nms
V_d	Con	Displacement volume (all cylinders)	m^3

Table 7.2: Abbreviations used in this report.

Abbreviation	Explanation
Con	Constant
Var	Variable
rpm	Revolutions per minute
S6	Scania's engine control system
OBD	On Board Diagnostics

Table 7.3: Indices used in this report.

Index	Explanation
im	Inlet manifold
em	Exhaust manifold
em2	Between the turbines
es	Exhaust system
trb1	Compressor turbine
trb2	Compound turbine
cmp	Compressor
eng	Engine
amb	Ambient
in	Into the component
out	Out of the component